Fluorine-18-Labeled Fluoroboronophenylalanine PET in Patients with Glioma

Yoshio Imahori, Satoshi Ueda, Yoshio Ohmori, Tsukasa Kusuki, Koji Ono, Ryou Fujii and Tatsuo Ido

Department of Neurosurgery, Kyoto Prefectural University of Medicine, Kyoto; Kyoto University Research Reactor Institute, Osaka; Cyclotron Unit, Nishijin Hospital, Kyoto; and Cyclotron and RI Center, Tohoku University, Sendai, Japan

We synthesized fluorine-18-labeled fluoroboronophenylalanine (^{18}F-^{10}B-FBPA), an analog of boronophenylalanine (^{10}B-BPA), and characterized its pharmacokinetics in patients with glioma. We conducted PET studies on three types of gliomas to clarify the relationship between tumor grade and each rate constant [K1 (ml/g/min), k2 (min^{-1}) and k3 (min^{-1})], and here, we discuss the metabolism of the ^{10}B-BPA analog (^{18}F-^{10}B-FBPA). **Methods:** Thirty-three cases of primary gliomas were studied by dynamic PET using DL-^{18}F-^{10}B-FBPA or L-^{18}F-^{10}B-FBPA. Dynamic PET images of ^{18}F-^{10}B-FBPA incorporation into tumors were obtained, and the arterial blood samplings were performed in all cases. **Results:** When the dynamic PET data were represented as Gjedde–Patlak plots, there was a positive slope, suggesting the involvement of the putative metabolic pool of this tracer. A three-compartment model using rate constants (K1, k2 and k3) was used for the kinetic analysis. The accumulation of ^{18}F-^{10}B-FBPA was found to correlate with the degree of malignancy, and the L form of ^{18}F-^{10}B-FBPA was taken up better than was the DL form. The results of dynamic PET analysis suggested that K1 (measuring amino acid transport process) is a major factor determining the accumulation of ^{18}F-^{10}B-FBPA. A comparison of the rate constants revealed that k3 (metabolic process) did not correlate with the degree of malignancy. The absence of evident differences in k3 between DL and L forms suggests that k3 represents phenomena that are not dependent on the native form of L. **Conclusion:** These PET data will be of practical use for diagnosis of malignancy and direct prediction of the effectiveness of boron neutron capture therapy using ^{10}B-BPA.

Key Words: fluoroboronophenylalanine; PET; boron neutron capture therapy

J Nucl Med 1998; 39:325–333

Boron neutron capture therapy (BNCT) for glioblastoma is receiving renewed attention (*1,2*) because extended resection of glioblastoma is not possible and because it is quite difficult to selectively kill just the infiltrative tumor tissue without injuring the brain itself. Boron neutron capture therapy allows ^{10}B to selectively accumulate in infiltrative brain tumor cells, and these cells can then be killed by the alpha rays that are generated by the nuclear reaction of thermal neutrons to ^{10}B (*3,4*). Theoretically, this is the optimal method for treating infiltrative malignant tumors. Boron-10-labeled boronophenylalanine (^{10}B-BPA) has been used to examine the efficacy on experimental animals with brain tumors (*5,6*), and it has also been used clinically for melanoma treatment (*7*). Our BNCT program is aimed at optimizing the treatment of glioblastoma using PET with ^{10}B-BPA serving as the boron carrier (*8,9*). However, the data on the pharmacokinetics of ^{10}B-BPA are not sufficient and have not been standardized. This is because direct pharmacokinetic analysis in ^{10}B in human glioma using ^{10}B-BPA is practically impossible. That is, continuous measurement of the tumor tissue ^{10}B in vivo is technically difficult. It is, therefore, desirable to develop techniques for continuous measurement of the tumor tissue ^{10}B levels using radioactive analogs of ^{10}B. We synthesized fluorine-18- and boron-10-labeled fluoroboronophenylalanine (^{18}F-^{10}B-FBPA) in two forms (DL-^{18}F-^{10}B-FBPA and L-^{18}F-^{10}B-FBPA) (*10*) and analyzed its kinetics using PET, which has been widely used for the in vivo diagnosis of various tumors to determine their three-dimensional and quantitative characteristics (*11*). We conducted PET studies on three types of gliomas to clarify the relationship between tumor grade and each rate constant [K1 (ml/g/min), k2 (min^{-1}) and k3 (min^{-1})] and, here, we discuss the metabolism of the ^{10}B-BPA analog (^{18}F-^{10}B-FBPA) in the human brain tumor.

Received Oct. 22, 1996; revision accepted May 6, 1997.

For correspondence or reprints contact: Yoshio Imahori, MD, PhD, Department of Neurosurgery, Kyoto Prefectural University of Medicine, Kawaramachi-Hirokoji, Kamigyo-ku 602, Kyoto, Japan.

MATERIALS AND METHODS

Synthesis of DL-Fluorine-18-Boron-10-Fluoroboronophenylalanine and L-Fluorine-18-Boron-10-Fluoroboronophenylalanine

We produced $^{18}F_2$ gas using a cyclotron (located at Nishijin Hospital, Kyoto, Japan), based on the atomic reaction $^{20}Ne(d,\alpha)^{18}F$, by bombarding a gaseous mixture of 99.5% Ne gas and 0.5% F_2 gas with accelerated deuterons. Carrier F_2 gas (150 μmol) was contained in neon target gas. This $^{18}F_2$ gas was used to synthesize ^{18}F-^{10}B-FBPA by a method using acetylhypofluorite (*10*). DL-3-(p-Boronophenyl)alanine (95% ^{10}B) and L-3-(p-boronophenyl)alanine (95% ^{10}B) were purchased from Boron Biologicals, Inc. (Raleigh, NC). Either DL-^{10}B-Boronophenylalanine or L-^{10}B-BPA (30 mg) was dissolved in 6 ml of trifluoroacetic acid, and acetylhypofluorite was bubbled into the trifluoroacetic acid solution. After trifluoroacetic acid was evaporated under reduced pressure, fluorine-18 adducts were dissolved in 2 ml of 0.1% acetic acid, and ^{18}F-^{10}B-FBPA was purified by separative radio high-performance liquid chromatography (HPLC). For separative HPLC, a Delta Pak (25 mm × 100 mm; Waters) column was used at room temperature. We used an eluent solvent of 0.1% acetic acid, and the flow rate was 10 ml/min. The elution time of ^{18}F-^{10}B-FBPA was 16 min under these conditions. After separation, acetic acid (0.1%) was evaporated and dissolved in 15 ml of saline. Finally, ^{18}F-^{10}B-FBPA solution was prepared by filtration using a Millipore filter (Millex-GS, 0.22μm; Waters). The ^{18}F-^{10}B-FBPA was then tested for pH and aseptic and pyrogenic properties before being used clinically. Quality control was performed as follows. We used a Nova pak C18 (8 mm × 100 mm; Waters) column for an analytical HPLC system at room temperature. The eluent system consisted of methyl alcohol:0.8% acetic acid containing 1 m*M* EDTA and 1 m*M* octylsulfate, 15:85 (v/v), as mobile phase for analysis of ^{18}F-^{10}B-FBPA. The flow rate was 2 ml/min, and the elution time was 8 min. The specific activity was 3.6 mCi/μmol. The radiochemical purity was more than 98%. The chemical structures are shown in Figure 1. Human application of the ^{18}F-^{10}B-FBPA-PET study and quality control of ^{18}F-^{10}B-FBPA (DL-^{18}F-^{10}B-FBPA and L-^{18}F-^{10}B-FBPA) followed the guidelines

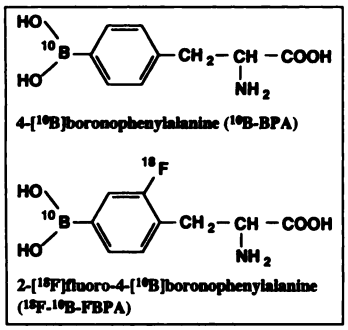

FIGURE 1. Chemical structures of ^{10}B-BPA and ^{18}F-^{10}B-FBPA.

established by the PET Committee of Nishijin Hospital (Kyoto, Japan) in January 1991.

Patients

The subjects consisted of 33 patients with primary brain tumor (Table 1), all of whom had been diagnosed as having glioma in our hospital between 1991 and 1996. Operations were performed for all of the patients, and in each case, as shown in Table 1, the diagnosis was confirmed histologically. Histological findings on the degree of malignancy were classified according to the World Health

TABLE 1
Kinetic Parameters and Tumor-to-Normal Ratios in Patients with Glioma*

Grade	Case no.	DL/L	K_1	k_2	k_3	k_4	θ	β	γ	T/N ratio
GBM	1044	DL	0.026	0.047	0.014	0.002	0.026	0.339	0.007	3.64
	1049	DL	0.03	0.072	0.038	0.01	0.026	0.17	0.01	3.74
	1094	DL	0.022	0.035	0.03	0.018	0.021	0.155	0.011	3.04
	1105	DL	0.017	0.021	0.035	0.015	0.017	0.122	0.011	3.42
	1139	DL	0.038	0.038	0.029	0.023	0.036	0.308	0.017	4.17
	2015	DL	0.027	0.031	0.026	0.011	0.026	0.264	0.014	3.64
Mean ± s.d. (n = 6)			0.027 ± 0.007	0.041 ± 0.018	0.029 ± 0.008	0.013 ± 0.007	0.025 ± 0.006	0.226 ± 0.089	0.012 ± 0.003	3.61 ± 0.37
AIII	1028	DL	0.033	0.048	0.02	0.004	0.033	0.26	0.013	3.04
	1093	DL	0.015	0.013	0.017	0.004	0.014	0.145	0.009	2.53
	1144	DL	0.014	0.015	0.025	0.009	0.014	0.125	0.01	3.23
	1156	DL	0.022	0.037	0.039	0.009	0.022	0.139	0.011	3.02
	1121	DL	0.053	0.034	0.013	0.009	0.051	0.482	0.022	5.15
	2085	DL	0.019	0.046	0.017	0.01	0.018	0.192	0.007	1.66
Mean ± s.d. (n = 6)			0.026 ± 0.015	0.032 ± 0.015	0.022 ± 0.009	0.008 ± 0.003	0.025 ± 0.014	0.224 ± 0.136	0.012 ± 0.006	3.11 ± 1.15
AII	1131	DL	0.005	0.006	0.017	0.01	0.005	0.037	0.004	1.01
	1189	DL	0.004	0.007	0.005	0.004	0.004	0.068	0.002	1.66
	2001	DL	0.003	0.01	0.031	0.005	0.003	0.02	0.003	0.8
	2047	DL	0.005	0.007	0.021	0.005	0.005	0.034	0.004	1.45
	2031	DL	0.008	0.019	0.027	0.009	0.008	0.069	0.005	1.73
Mean ± s.d. (n = 5)			0.005 ± 0.002	0.010 ± 0.005	0.020 ± 0.010	0.007 ± 0.003	0.005 ± 0.002	0.046 ± 0.022	0.003 ± 0.001	1.33 ± 0.41
Control (n = 17)		DL	0.006 ± 0.002	0.020 ± 0.013	0.031 ± 0.020	0.010 ± 0.006	0.005 ± 0.002	0.033 ± 0.018	0.004 ± 0.001	
GBM	2108	L	0.041	0.028	0.02	0.004	0.042	0.45	0.02	3.82
	2121	L	0.045	0.049	0.013	0.004	0.043	0.584	0.01	3.22
	4069	L	0.029	0.03	0.022	0.009	0.029	0.288	0.013	2.07
	4073	L	0.032	0.022	0.027	0.011	0.031	0.276	0.019	4.46
	4078	L	0.051	0.036	0.029	0.009	0.05	0.437	0.023	2.62
	4115	L	0.043	0.022	0.004	0.015	0.04	0.821	0.014	3.05
	5058	L	0.05	0.04	0.017	0.024	0.048	0.59	0.015	3.35
Mean ± s.d. (n = 7)			0.041 ± 0.008	0.033 ± 0.010	0.019 ± 0.009	0.011 ± 0.007	0.042 ± 0.008	0.492 ± 0.191	0.016 ± 0.004	3.23 ± 0.78
AIII	2171	L	0.037	0.026	0.048	0.007	0.031	0.281	0.018	2.24
	3027	L	0.088	0.047	0.027	0.011	0.081	0.714	0.031	3.67
	3111	L	0.02	0.022	0.027	0.004	0.019	0.166	0.011	1.55
	3134	L	0.03	0.011	0.003	0.015	0.029	0.145	0.022	3.82
	5040	L	0.027	0.038	0.025	0.023	0.026	0.218	0.012	2.45
	6010	L	0.034	0.035	0.023	0.005	0.033	0.307	0.014	3.13
Mean ± s.d. (n = 6)			0.039 ± 0.025	0.030 ± 0.013	0.025 ± 0.014	0.011 ± 0.007	0.037 ± 0.022	0.305 ± 0.210	0.018 ± 0.008	2.81 ± 0.88
AII	2127	L	0.016	0.025	0.03	0.007	0.015	0.127	0.009	1.89
	5071	L	0.031	0.034	0.025	0.009	0.031	0.301	0.013	1.95
	5077	L	0.022	0.032	0.02	0.009	0.022	0.224	0.01	1.88
Mean ± s.d. (n = 3)			0.023 ± 0.008	0.030 ± 0.005	0.025 ± 0.005	0.008 ± 0.001	0.023 ± 0.008	0.217 ± 0.087	0.011 ± 0.003	1.91 ± 0.04
Control (n = 16)		L	0.011 ± 0.003	0.025 ± 0.010	0.033 ± 0.015	0.009 ± 0.011	0.011 ± 0.003	0.084 ± 0.036	0.006 ± 0.002	

*Of the 33 patients, 17 were studied using DL-^{18}F-^{10}B-FBPA, and 16 were studied using L-^{18}F-^{10}B-FBPA. Patients of both groups were categorized as GBM, AIII or AII. Values of the rate constants (K_1, k_2, k_3 and k_4) are given as mean ± s.d. θ and K1 are equivalent in theorem. β is tracer-distribution volume (D_v). γ is a degree of the accumulation rate (min^{-1}). A control was established at the corresponding region in contralateral white matter in each case.

Organization (WHO) committee grading criterion (AII, astrocytoma WHO grade II; AIII, anaplastic astrocytoma WHO grade III; GBM, glioblastoma multiforme). Conventional CT (x-irradiation CT) images were obtained for comparison for each case before the PET studies.

Methods of Dynamic PET Study

The spatial resolution in PET was 8.6 mm in FWHM in-plane resolution, and the average axial resolution was 13.6 mm. x-irradiation CT and MRI were performed on all of the patients. No patients had a history of other malignant diseases. Dynamic images of ^{18}F-^{10}B-FBPA incorporation into tumors were obtained using PET in all cases. PET scans were conducted with a tomograph using the Headtome III (Shimadzu Co., Kyoto, Japan). The planes of the PET scans were set to be the same as those in the parallel CT studies. Local cerebral blood volume (CBV) was measured after bolus inhalation of ^{15}O-labeled carbon monoxide gas (*12*). Fluorine-18-boron-10-fluoroboronophenylalanine (1–1.5 mCi per 10 kg body weight) was injected intravenously for 40 sec. The starting time of the dynamic PET study was set at that time when the whole-brain activity reached a value greater than that of the background activity. PET data were collected continuously for 9 2-min periods and 6 4-min periods, making a total of 15 periods for a total of 42 min (Fig. 2A). The four initial arterial blood samples were obtained at 5-sec intervals with the following samples obtained at gradually longer intervals (0.5 min–10 min), making a total of 21 samples in a period of 42 min (Fig. 2B). We set the PET counting area (region of interest, or ROI) with 49–171 pixels (1 pixel = 2 mm × 2 mm) on the tumor center and the nontumoral control area. All macroscopically necrotic tumor areas were excluded when ROIs were designated. We had confirmed that the radioactivity distributions in each pixel within the ROIs had s.d. values below 18%. Using this as a criterion, we limited macroscopic heterogeneity to a minimum when designating ROIs. The ROI images were composed of 49–171 pixels and, hence, had a minimum voxel volume of 2.94 cm^3. Cases in which the hot area (active area) was smaller than the above-mentioned area were excluded from the evaluation. The tumor areas of all 33 cases presented here satisfied this requirement of voxel volume. No particular partial volume corrections were performed on any cases. We designated several ROIs from tumor-affected areas and adopted the region with highest values as a representative ROI.

Correction of PET Data by Cerebral Blood Volume

In each study, we corrected for overestimation of ^{18}F-^{10}B-FBPA incorporation by CBV. The correction was performed according to the following equation (*13*):

$$C_i^{PET}(t) = (1 - CBV)C_i(t) + w \cdot CBV \cdot C_p(t), \qquad \text{Eq. 1}$$

where $C_i(t)$ is the CBV-corrected real ^{18}F tissue time–activity data in the ROI, $C_i^{PET}(t)$ is the ^{18}F tissue time–activity data obtained by positron camera, CBV is the CBV measured by ^{15}O-labeled carbon monoxide gas, w is the ratio of ^{18}F-^{10}B-FBPA radioactivity in whole blood to that in plasma and $C_p(t)$ is the plasma time–activity curve as an input function obtained by actual measurement by arterial sampling. A comment about w is discussed below.

Three-Compartment Model and Gjedde–Patlak Plot

Our preliminary data obtained by dynamic PET studies using ^{18}F-^{10}B-FBPA suggested that the time–activity curves showed a characteristic accumulation of the ^{18}F activity. After rapid increase for the quasi-steady-state period, the accumulation remained stable (Fig. 2A). When the dynamic PET data were represented as Gjedde–Patlak plots (*14*), there was a positive slope, suggesting the involvement of the putative metabolic pool of this tracer. Therefore, the pharmacokinetics of ^{18}F-^{10}B-FBPA were analyzed using

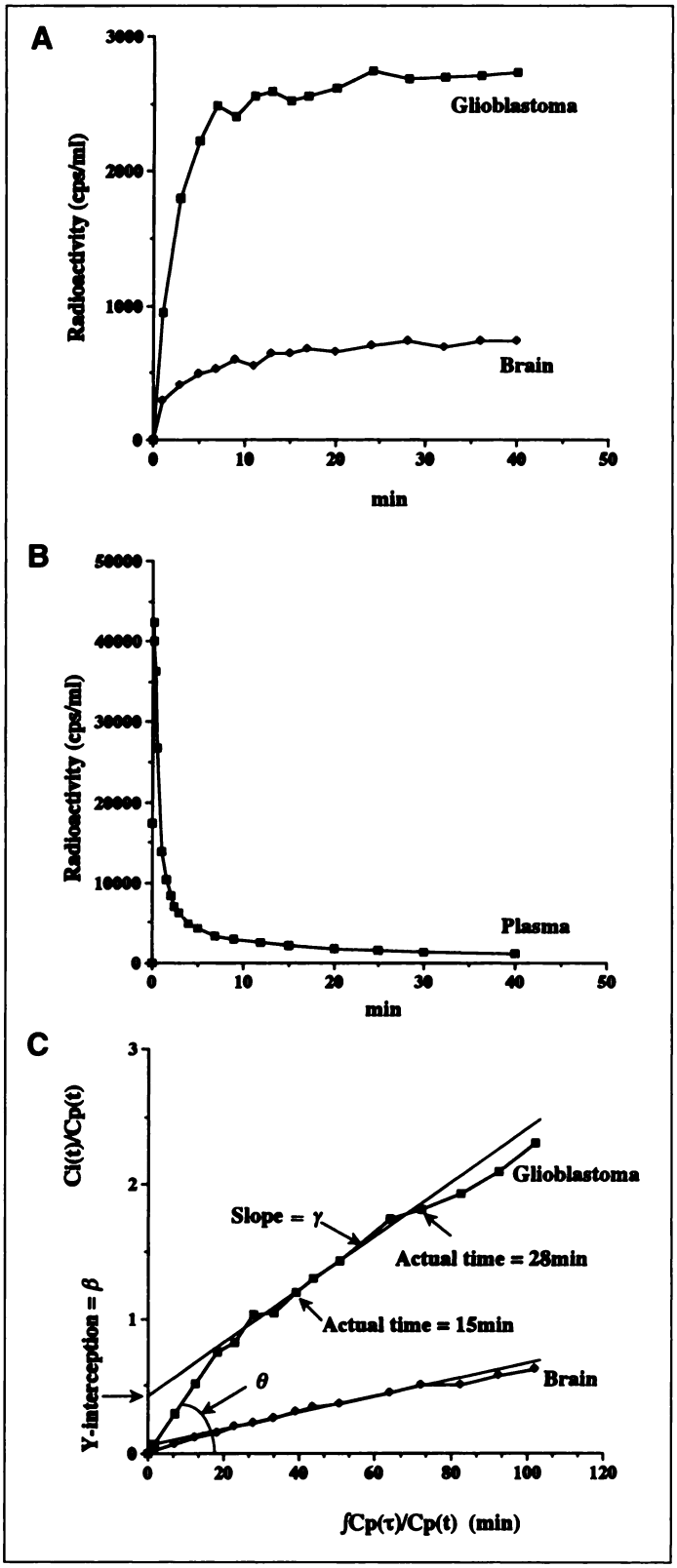

FIGURE 2. Dynamic PET studies using L-^{18}F-^{10}B-FBPA in patient with glioblastoma. (A) The time–activity curves, $C_i(t)$, obtained by a dynamic PET. (B) The input function, $C_p(t)$, obtained by arterial blood sampling. (C) Gjedde–Patlak plot to derive the parameters θ, β and γ.

the three-compartment model, with K1 (ml/g/min), k2 (min^{-1}) and k3 (min^{-1}). The details about a compartment model for ^{18}F-^{10}B-FBPA uptake are discussed below. The following equation, which includes k4 (min^{-1}) and was proposed by Huang et al. (*15*), is a generalized model of the theorem of the three-compartment model:

$$C_i(t) = \frac{K_1}{(\alpha_2 - \alpha_1)}[(k_3 + k_4 - \alpha_1)e^{-\alpha_1 t} + (\alpha_2 - k_3 - k_4)e^{-\alpha_2 t}] \otimes C_p(t)$$
$$\alpha_1 = [(k_2 + k_3 + k_4) - \sqrt{(k_2 + k_3 + k_4)^2 - 4k_2k_4}]/2 \quad \text{Eq. 2}$$
$$\alpha_2 = [(k_2 + k_3 + k_4) + \sqrt{(k_2 + k_3 + k_4)^2 - 4k_2k_4}]/2$$

The nonlinear least square best regression method was adopted to obtain the rate constants (K1, k2, k3 and k4). However, no reference data for these rate constants have been reported, and we encountered some problems when using the initial values required to perform the best regression method. When the regression process was minimized, there were some peripheral minimum values corresponding to the initial values of the rate constants. To perform accurate estimation of the rate constants, the optimal initial values should be defined. Thus, we used the Gjedde–Patlak graphic method (*14*) to derive the parameters θ, β and γ to solve this problem (Fig. 2C).

Assuming k4 to be zero, the solution for the three-compartment model as expressed by Gjedde–Patlak plotting is as follows:

$$C_i(t) = \frac{K_1}{(k_2 + k_3)}\left[k_3\int_0^t C_p(\tau)d\tau + k_2e^{-(k_2+k_3)t} \cdot \int_0^t C_p(\tau)e^{(k_2+k_3)\tau}d\tau\right] \quad \text{Eq. 3}$$

$$\frac{C_i(t)}{C_p(t)} = \frac{K_1k_3}{(k_2 + k_3)}\left[\frac{\int_0^t C_p(\tau)d\tau}{C_p(t)}\right] + \frac{K_1k_2}{(k_2 + k_3)^2}. \quad \text{Eq. 4}$$

There is an indication in Equation 4 that it should be applied when plasma and the reversible compartment are in equilibrium. This equation expresses the relationship between $C_i(t)/C_p(t)$ and $\int_0^t C_p(\tau)d\tau/C_pt$. This can be considered the first-order function. The parameters θ, β and γ can be obtained by delineation of the tangent on the plotting, as follows:

$$\theta = \lim_{t\to 0} C_i(t) \Big/ \int_0^t C_p(\tau)\, d\tau$$
$$\beta = K_1k_2/(k_2 + k_3)^2 \quad \text{Eq. 5}$$
$$\gamma = K_1k_3/(k_2 + k_3).$$

θ and K1 are equivalent in theorem. β is an indicator of the global accumulation of ^{18}F-^{10}B-FBPA as tracer distribution volume (D_v). A degree of the accumulation rate of the tracer is reflected in γ value.

This parameter set can be solved for K1, k2 and k3 as follows:

$$K_1 = \theta$$
$$k_2 = \frac{\theta(\sigma - 1)^2}{\beta\sigma^2}$$
$$k_3 = \frac{\theta(\sigma - 1)}{\beta\sigma^2}, \quad \text{Eq. 6}$$

with

$$\sigma = \frac{\theta}{\gamma}.$$

These should be the initial rate constant values for each case. The regression process was minimized when they were used. In cases in which the k4 was comparatively high, there was a tendency for the β value to be overestimated and for the γ value to be underestimated. Accordingly, we obtained the tangent line by establishing a best-fit area on each Gjedde–Patlak plot, from 15 min to 28 min (as actual time) because linearity was well-maintained within this range and then deriving from this segment (Fig. 2C).

Plasma Metabolites of Fluorine-18-Boron-10-Fluoroboronophenylalanine

A previous report demonstrated that labeled metabolites within the arterial plasma were present in small amounts during 1-hr animal experiments (*16*). In our human PET studies, the metabolic fractions were negligible for 42 min because we observed that >95% of the total radioactivity of the plasma was free ^{18}F-^{10}B-FBPA during the 42-min arterial sampling. These data suggest that plasma metabolite correction is not necessary.

Statistical Methods

F-distribution values for each of the contribution factors were derived based on analysis of variance (ANOVA). Two-factor factorial ANOVA was used to assess whether or not the glioma grade and the form (DL or L) of ^{18}F-^{10}B-FBPA would determine each kinetic constant. The multiple comparison procedure was performed by Scheffe's F-method. These values were then used to produce the p value, which expresses the possibility of positive discrimination of the prominent factors.

RESULTS

Tumor Imaging Using Fluorine-18-Boron-10-Fluoroboronophenylalanine

Figure 3 shows typical dynamic PET studies using DL- or L-^{18}F-^{10}B-FBPA in patients with gliomas (Cases 1094 and 2171 in Table 1). The PET images demonstrate a gradual incorporation profile in the lesions (Fig. 3, C and F). The activity then remained at a constant level after 30 min (lesion profiles 34, 37, 40 and 43 in Fig. 3C and 35, 38, 41 and 44 in Fig. 3F). We can see a more extensive area incorporating ^{18}F-^{10}B-FBPA (Fig. 3B) than that of MRI with Gd enhancement (Fig. 3A). The PET data revealed that DL-^{18}F-^{10}B-FBPA was actively incorporated to the malignant tumor cells, showing high radioactivity and tumor-to-normal ratio (T/N ratio) (Table 1). In Case 2171, the active area seen in the PET image (Fig. 3E) is in marked contrast to the findings seen in MRI with Gd enhancement. There was no Gd enhancement in the lesion corresponding to the active area (Fig. 3D).

Arterial Plasma Sampling

Regarding the ratio of ^{18}F-^{10}B-FBPA radioactivity in whole blood to that in plasma, we followed the time course of both whole blood and plasma radioactivity determined in parallel (n = 9). As shown in Figure 4, the w value, i.e., the blood-to-plasma ratio of radioactivity, changed little with time. On the basis of this result, we judged it reasonable to treat w as a constant in this test, which lasted 42 min (w = 0.7).

Pharmacokinetics of Fluorine-18-Boron-10-Fluoroboronophenylalanine in Human Gliomas

The pharmacokinetics of ^{18}F-^{10}B-FBPA were examined using a dynamic PET study. When the data were represented as Gjedde–Patlak plots, there was a positive slope (Table 1, γ values), suggesting the involvement of one-way (unidirectional) transfer and accumulation of the tracer. This indicated that a three-compartment model using rate constants (K1, k2 and k3) was used for the kinetic analysis. Table 1 shows the K1, k2, k3, k4, θ, β and γ values obtained from all glioma cases. According to the nonlinear least squares best regression method using the initial rate constant values, good approximation was observed

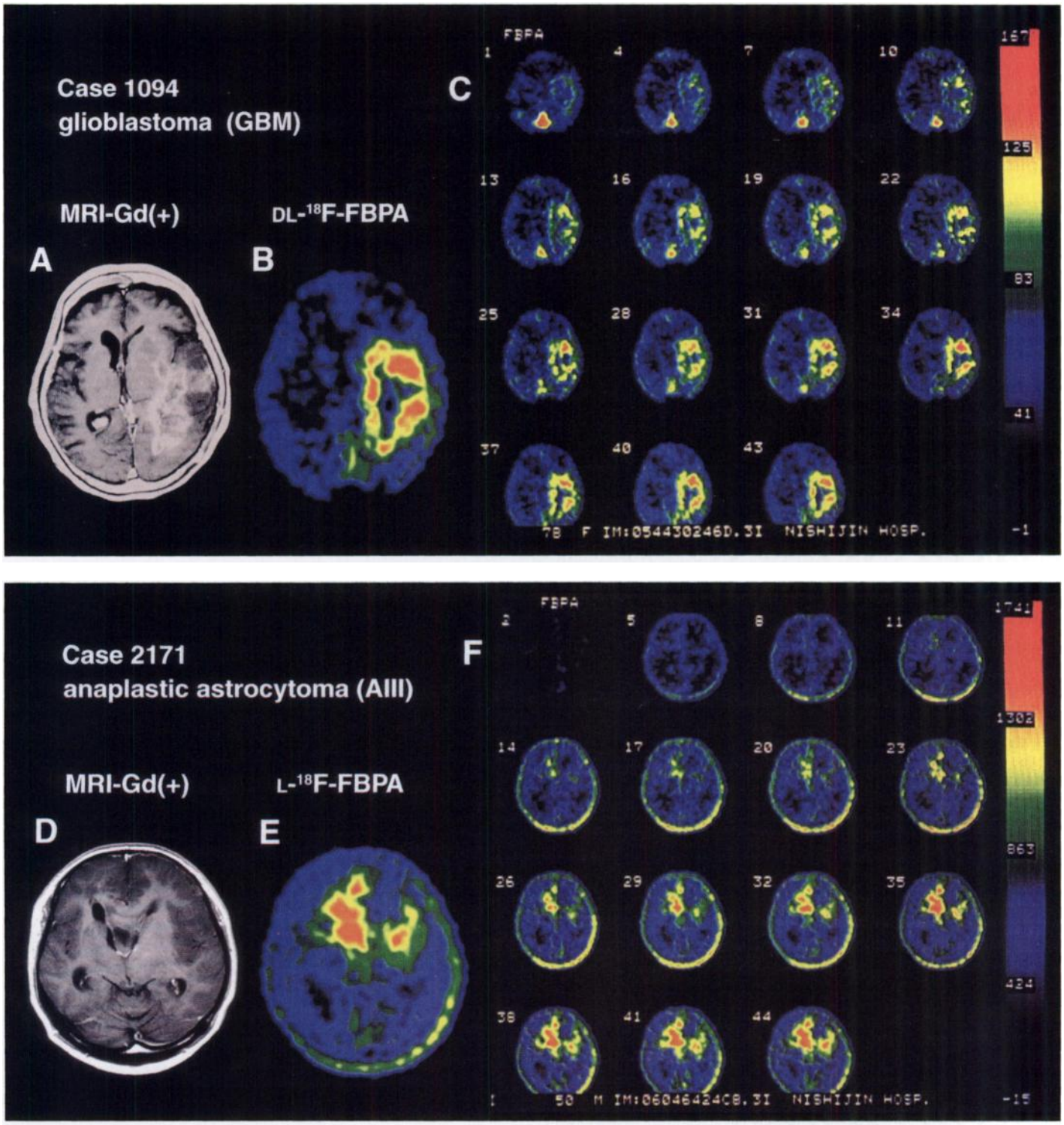

FIGURE 3. Typical PET images of ^{18}F-^{10}B-FBPA in patients with gliomas. Typical dynamic PET studies using DL- and L-^{18}F-^{10}B-FBPA in patients with glioblastoma (A–C, Case 1094) and anaplastic astrocytoma (D–F, Case 2171) are shown. (A and D) MRI with Gd enhancement. (B and E) PET images corresponding to the MRI. (C and F) Dynamic PET study using ^{18}F-^{10}B-FBPA in patients with gliomas. A sequential scanning was performed nine times at 2-min intervals and six times at 4-min intervals. The total examination took 42 min.

between the K1 and θ values. We decided to omit evaluating k4 values because of their minimal significance. Figure 5 shows the results of the K1, k2 and k3 values of each form (D/L and L).

Factorial Analysis of Variance of Glioma Grade and DL/L Forms

Two-factor factorial ANOVA showed that both the glioma grade ($p < 0.0001$) and DL/L form of ^{18}F-^{10}B-FBPA ($p < 0.0001$) served as K1 determinants. As shown in Table 2, Scheffe's test was used to examine the difference in K1 between different grades of glioma at a significance level of 0.05. This indicated that K1 is closely related to ^{18}F-^{10}B-FBPA uptake, which correlates with the degree of malignancy (inter-grade correlation by Scheffe's test; GBM–AIII, $p = 0.97$; GBM–AII, $p < 0.0001$; GBM–control, $p < 0.0001$; AIII–AII, $p = 0.0002$; AIII–control, $p < 0.0001$; and AII–control, $p = 0.82$). k2 was found to be a determinant of glioma grade ($p < 0.002$) but not the DL/L form ($p < 0.30$). Scheffe's test, at a significance level of 0.05, indicated that k2 is slightly related to

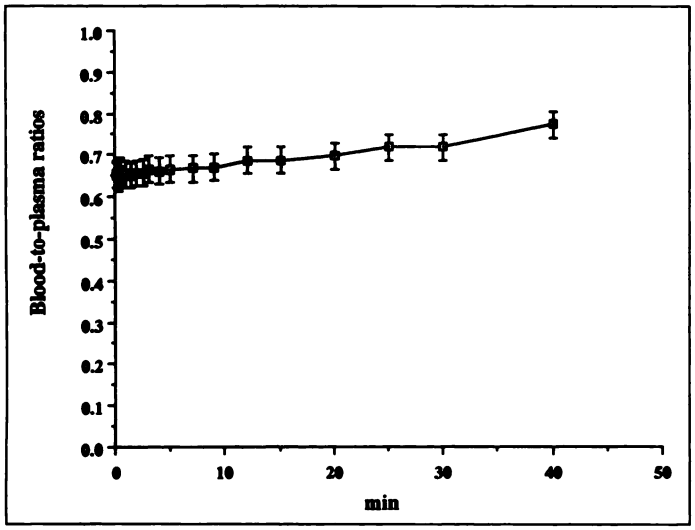

FIGURE 4. Time course of blood-to-plasma ratios. In glioma cases (n = 9), we followed the time course of both whole blood and plasma radioactivity, determined in parallel in L-^{18}F-^{10}B-FBPA studies. As shown in this figure, the blood-to-plasma ratios of radioactivity (w) change little with time.

^{18}F-^{10}B-FBPA uptake, which correlates with the degree of malignancy (GBM–AIII, p = 0.75; GBM–AII, p < 0.011; GBM–control, p = 0.011; AIII–AII, p = 0.12; AIII–control, p = 0.23; and AII–control, p = 0.77). Two-factor factorial ANOVA revealed k3 was not a determinant of either DL/L form or the glioma grade (p = 0.96 and 0.17, respectively). At a significance level of 0.05, there was no significant intergrade difference in k3. Two-factor factorial ANOVA revealed that both glioma grade and the DL/L form served as determinants of both β and γ values (p < 0.0001), as shown in Table 2.

Tumor-to-Normal Ratios

The T/N ratios shown in Figure 6 were calculated from the cps/ml on the images, without correction for CBV. As shown in Figure 6, 20 min or more after injection, time no longer determined the T/N ratios, and they became steady. Therefore, the T/N ratio after 20 min can be regarded as a tumor's characteristic constant. This is probably because an equilibrium was established between the tumor and the brain. We used the mean value obtained from three later sequential images (30–34 min, 34–38 min and 38–42 min) as a proper T/N ratio for a patient (Table 1). Using factorial ANOVA, we found that glioma grade was a determinant of the T/N ratio and the DL/L form did not affect the T/N ratio, as shown in Table 2. The T/N ratio can be used as a reliably stable indicator of the glioma grade. When tested using the Student's t-test, the T/N ratio in GBM cases and AIII cases did not differ significantly between DL and L forms (p = 0.2 and 0.78, respectively). This suggests that in the malignant group indicated for BNCT, the T/N ratio does not differ between DL and L forms (Table 2). Thus, cases can be regarded as being malignant group if the T/N ratio is higher than 2.

DISCUSSION

Input Function of Fluorine-18-Boron-10-Fluoroboronophenylalanine and Tumor Cerebral Blood Volume Measurement

Regarding the metabolites in the plasma, it was reported by Ishiwata et al. (*16*) that the radioactivity is gradually incorporated into the acid-insoluble fractions in the plasma in animal experiments. However, only 6.3% of the total radioactivity of the plasma appeared in the acid-insoluble fractions within 1 hr, and most radioactivity in the acid-soluble fraction in plasma

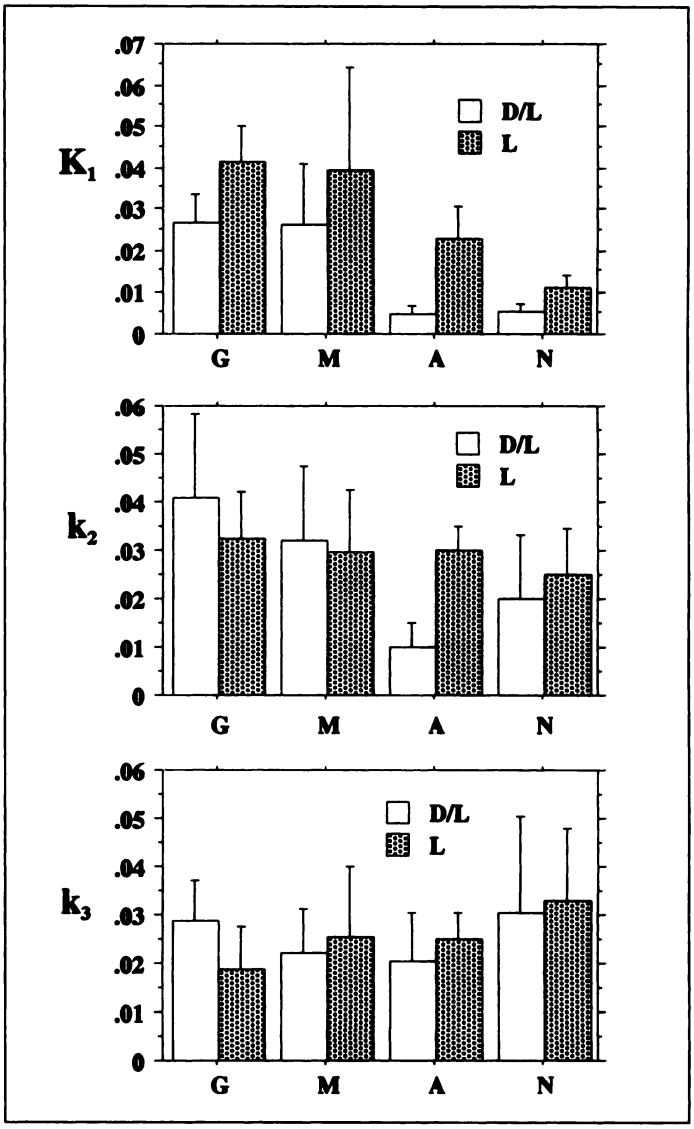

FIGURE 5. K1, k2 and k3 values of DL- and L-^{18}F-^{10}B-FBPA. Bar graph showing the values of each rate constant (K1, k2 and k3) of DL- and L-^{18}F-^{10}B-FBPA. Values are means ± s.d. G, glioblastoma; M, anaplastic astrocytoma; A, astrocytoma; N, normal brain.

was recovered as ^{18}F-^{10}B-FBPA (*16*). In our human PET studies, the metabolic fraction is negligible during the 42-min duration of the studies because we observed that >95% of the total radioactivity of the plasma was free ^{18}F-^{10}B-FBPA fraction during 42-min arterial sampling. Another problem is possible time dependence of the blood-to-plasma activity ratio. Figure 4 supports the assumption that an activity ratio w is implied to be time-independent. The CBV values are largely determined by the tumor drainer veins or compressed and dislocated surface veins. For this reason, caution should be used when accepting CBV as an indicator of tumor malignancy level. Because several reports have referred to the relationship between CBV and tumor malignancy (*17*), it does not seem to be important to discuss it here. In this study, CBV measurement was incorporated to elevate the accuracy of $C_i(t)$. When corrected by CBV, $C_i(t)$ can be measured more accurately, and it affects the measurement of the initial value of K1 significantly.

Compartment Model Analysis for Fluorine-18-Boron-10-Fluoroboronophenylalanine

Wienhard et al. (*13*) proposed a compartment model for [2-^{18}F]fluorotyrosine (^{18}F-fluorotyrosine) uptake with three or

TABLE 2
Effects on the Rate Constants (K_1, k_2 and k_3), β, γ and Tumor-to-Normal Ratios of the Glioma Grade and DL/L Form of Fluorine-18-Boron-10-Fluoroboronophenylalanine

Two-factor ANOVA	K_1	k_2	k_3	β	γ	T/N ratio
Effect of the glioma grade	<0.0001	<0.002	NS	<0.0001	<0.0001	<0.0001
Intergrade correlation						
GBM–AIII	NS	NS	NS	NS	NS	NS
GBM–AII	<0.0001	0.011	NS	<0.0001	<0.0001	<0.0001
GBM–Cont	<0.0001	0.011	NS	<0.0001	<0.0001	<0.0001
AIII–AII	0.0002	NS	NS	0.018	<0.0001	<0.0001
AIII–Cont	<0.0001	NS	NS	<0.0001	<0.0001	<0.0001
AII–Cont	NS	NS	NS	NS	NS	NS
Effect of DL/L form	<0.0001	NS	NS	<0.0001	<0.0001	NS
Interaction between grade and DL/L form	NS	NS	NS	<0.017	NS	NS

*Effects on each rate constant, β, γ and T/N ratio were examined by two-factor factorial ANOVA (the two factors were glioma grade and DL/L form). For effect of the glioma grade, intergrade correlations were obtained using Scheffe's F-method. These correlations were expressed by p values. Cont = normal brain; NS = not significant.

five rate constants. In this model, K1 and k2 refer to forward and reverse transport of ^{18}F-fluorotyrosine across the blood–brain barrier, respectively. The k3 is the rate constant for incorporation into proteins. Furthermore, the three rate constant model is extended to a five-parameter model by adding a further serial tissue compartment with inward and outward transport rate constants k3 and k4, respectively. The incorporation into proteins is then described by rate constant k5. In addition, this model for ^{18}F-fluorotyrosine is different from that for L-[1-^{11}C]tyrosine (^{11}C-tyrosine), with an extra metabolite compartment (*18*). The time–activity curves of ^{18}F-fluorotyrosine are quite different from those of [^{11}C]tyrosine. Because of the similar results of dynamic PET data of ^{18}F-^{10}B-FBPA and ^{18}F-fluorotyrosine, the five-parameter model was adopted. It is assumed that k5 is a negligible parameter (Fig. 7) because the ^{18}F-^{10}B-FBPA is probably reserved, without any metabolic alteration, in amino acid pool in the tumor tissue (*16,19,20*). Even if ^{18}F-^{10}B-FBPA cannot reflect anabolic process, it can be emphasized that our main purpose is to estimate tumor ^{10}B concentration for BNCT using the rate constants of ^{18}F-^{10}B-FBPA. Then this model is very similar to the deoxyglucose (DG) model, and the mathematical forms of the model equations are identical to the equations of Huang et al. (*15*).

Interpretation of K1 and k3

The K1 value differed significantly between the malignant group (GBM and AIII) and the benign group (AII), as shown in Table 2 and Figure 5. This difference was seen for both the DL and L forms of ^{18}F-^{10}B-FBPA. On the other hand, k3 did not differ between the two groups, nor was there a significant difference in k3 between the DL and L forms. These findings indicate that ^{18}F-^{10}B-FBPA uptake capacity, associated with tumor grade, is dependent on K1, which is an indicator of the transport process. No interactions between glioma grade and form were observed except in terms of β values (Table 2). This means that no undiscussed problems in interpretation of K1 and k3 are produced by interactions between glioma grade and form. The choice of DL or L form was found to determine K1 (Table 2). Because K1 is thought to be a quantitative parameter of the amino acid transport process, the L form is distinguished from the DL form during amino acid transport. Therefore, it is likely that amino acid transport, which is a biologically significant process (*21*), is represented by K1. Another parameter of k3, which is a putative metabolic process, was not dependent on

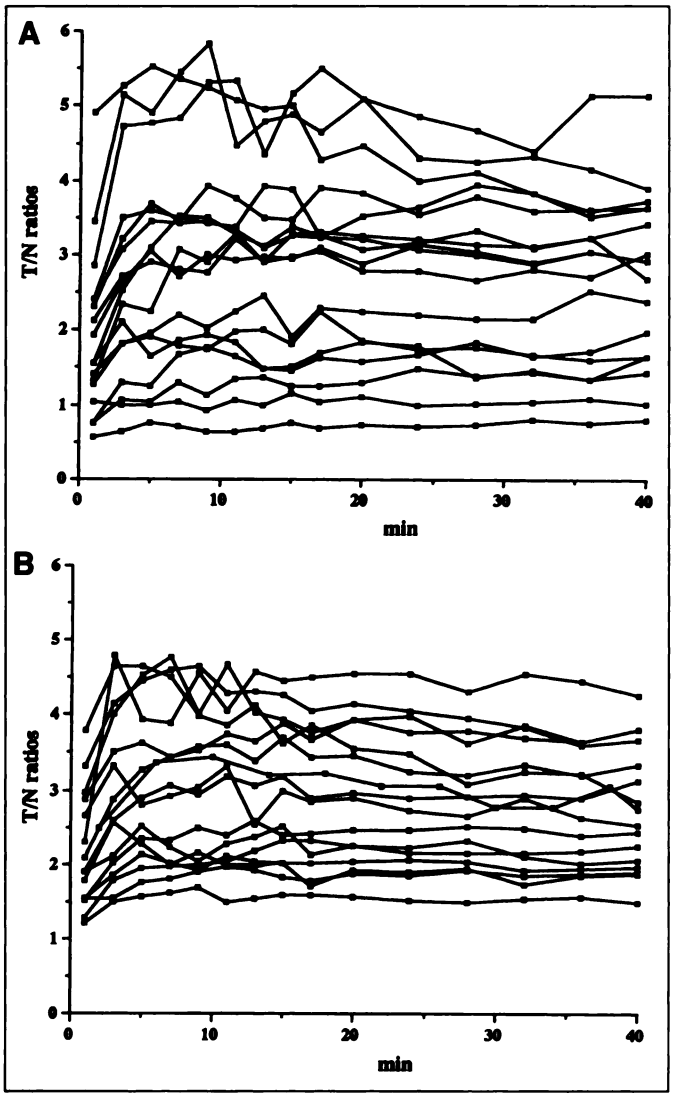

FIGURE 6. Time course of tumor-to-normal ratios of DL- and L-^{18}F-^{10}B-FBPA. The T/N ratio was calculated from cps/ml on each dynamic PET images, without correction for CBV using C^{15}O. (A) Time courses of T/N ratios of all types of gliomas studied using DL-^{18}F-^{10}B-FBPA. (B) Time courses of T/N ratios of all types of gliomas studied using L-^{18}F-^{10}B-FBPA. The T/N ratios reached equilibrium after 20 min, even when no correction was made. We used the mean value obtained from three later sequential images (30–34 min, 34–38 min and 38–42 min) as a proper T/N ratio for a patient.

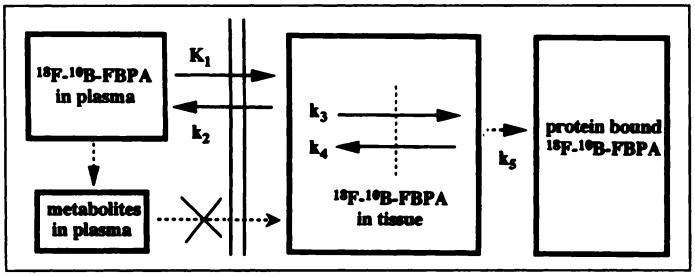

FIGURE 7. Compartment model for ^{18}F-^{10}B-FBPA uptake with four rate constants. This compartment model for ^{18}F-^{10}B-FBPA is modified from that for ^{18}F-tyrosine uptake, reported by Wienhard et al. (*13*). The five-parameter model was adopted for ^{18}F-^{10}B-FBPA uptake. K1 and k2 refer to forward and reverse transport of ^{18}F-^{10}B-FBPA across the blood–brain barrier, respectively. k3 represents some retention process in the second compartment (precursor pool) toward incorporation into proteins, and k4 represents the outward transport process. It is assumed that k5 is negligible parameter (dotted arrow) because the ^{18}F-^{10}B-FBPA is probably reserved, without any metabolic alteration, in amino acid pool in the tumor tissue. Then this model is very similar to the DG model, and the mathematical forms of the model equations are identical to the equations of Huang et al. (*15*). It is assumed that a small amount of metabolites in plasma does not cross the blood–brain barrier.

tumor grade or DL/L difference (Table 2 and Fig. 5). The absence of evident differences in k3 between DL and L forms suggests that k3 represents phenomena that are not dependent on the native form of L-^{18}F-^{10}B-FBPA. In other words, this process may not be due to any specific biological process. Although direct studies are needed on this issue, we speculate that ^{18}F is pooled within cells due to some retention mechanisms via the amino acid anabolic pathway rather than due to incorporation into proteins. This kinetic analysis demonstrated that the L form of ^{18}F-^{10}B-FBPA is taken up better by tumor tissue than is its DL form. Because the difference in form (DL or L) only determines K1, the amount of uptake is strongly dependent on K1. Because k2 is not affected by the difference in form (DL or L), the partition coefficient (K1/k2) is also dependent only on K1. In cases of GBM, for example, the average K1 for the L form was 1.5 times that for the DL form. Approximately the same magnitude of difference in average K1 was also noted when the concept "incorporation constant" was used for calculation (*8*). Both the DL and L forms of ^{18}F tracer are of similar value for diagnosing tumors. However, in the case of BNCT, in which the tumor tissue ^{10}B level is important, the L form of ^{10}B-BPA seems to be more suitable.

Parameters Obtained by Gjedde–Patlak Plot

β and γ, which are parameters based on K1, also reflected tumor grade well. β, which indicates the tracer distribution volume (D_v), correlated particularly well with tumor grade between GBM and AIII ($p < 0.102$ in Table 2). However, our data suggest some possible interactions between glioma grade and D/DL form. The interaction appears to be associated with blood–brain barrier breakdown. γ is as useful as K1 in discriminating among different grades. The average of γ, which is an indicator of the overall tracer uptake rate, was somewhat high in AIII cases in the L form (Table 1), probably because AIII cases are necrosis-free, unlike GBM. In terms of the parameter, there was no marked difference between GBM and AIII. These tendencies were seen irrespective of the use of DL or L form. We evaluated the accuracy and precision of estimating rate constants from Gjedde–Patlak plot. When the initial K1, k2 and k3 values (in Eq. 6), obtained from the Gjedde–Patlak plots, were compared with the real rate constants yielded from fitting, a good correlation was obtained as shown in Figure 8. This indicates that the rate constant images can be easily represented graphically by the use of the simple Equation 6.

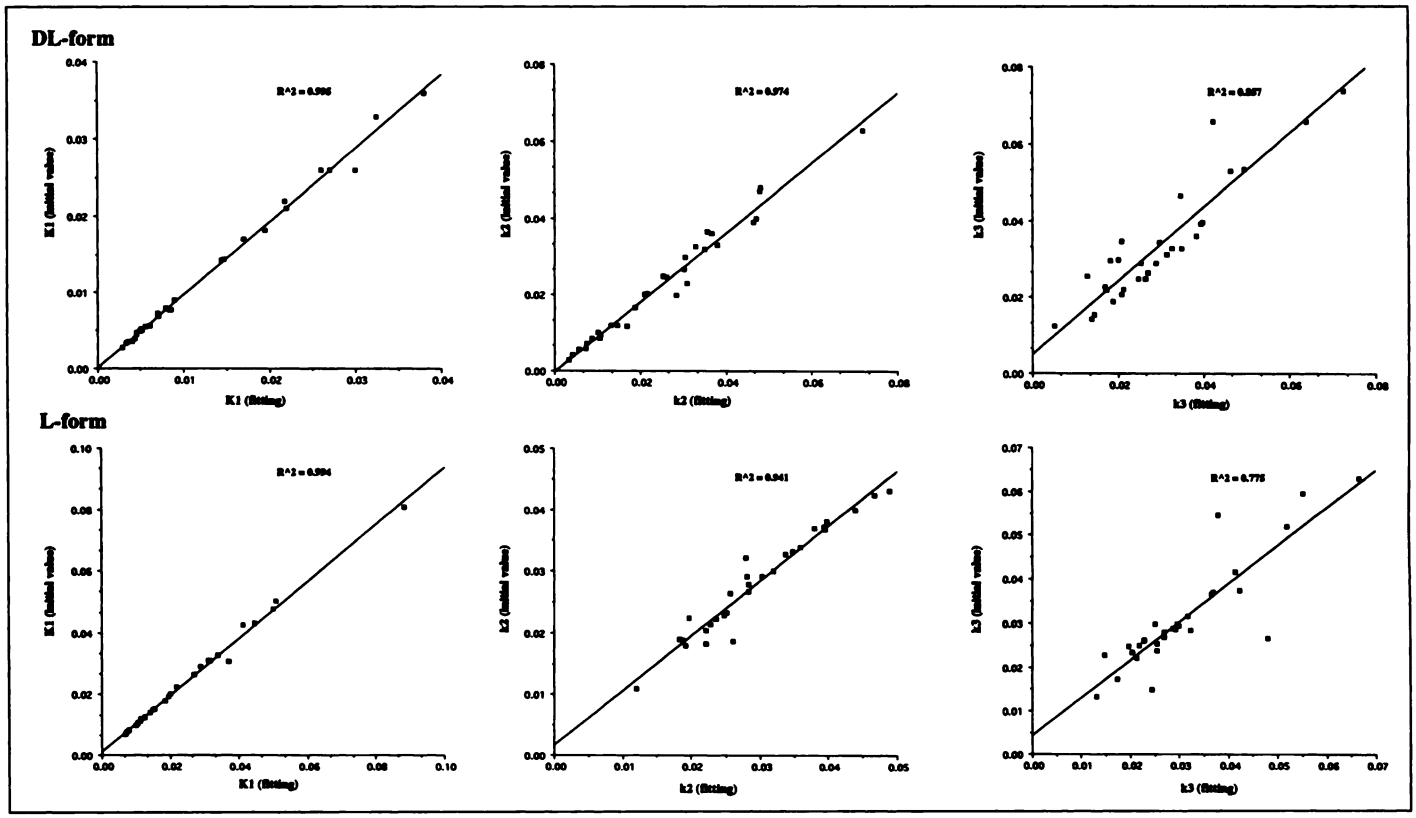

FIGURE 8. In each graph, plots include all cases of gliomas and normal brain studied by using DL- or L-^{18}F-^{10}B-FBPA. X-axes represent K1, k2 and k3 values obtained by the nonlinear least square best regression method, and Y-axes represent the initial K1, k2 and k3 values obtained by Equation 6. When the initial rate constants are compared with the real values, a good correlation is obtained from K1 and k2 in both DL and L forms. A slight dispersion is shown in k3.

Simple Tumor-to-Normal Ratio as a Useful Predictor of Malignancy of Gliomas

Another important factor for BNCT is the T/N ratio. Both normal brain tissue and glioma-affected tissue take up L-^{18}F-^{10}B-FBPA better than DL-^{18}F-^{10}B-FBPA. As a result, the T/N ratio does not differ between L- and DL-^{18}F-^{10}B-FBPA (Table 1). The ratio became constant after 20 min even when no correction was made (Fig. 6). As shown in Table 1, two patients with AIII, in whom the T/N ratios were 1.66 and 1.55, had long survival periods. Discrepancy between pathological diagnosis and the T/N ratio based on amino acid transport activity was seen in cases like these two. Cases with a T/N ratio of >2 followed unfavorable clinical courses. Because the number of cases with low-grade astrocytoma was small in this study, an additional analysis of sensitivity and specificity was needed. What was most important in this study was to characterize analogs of L-^{10}B-BPA before applying BNCT. The data we obtained allow us to conclude that patients with a T/N ratio of >2 should be considered for the application of BNCT.

Toward the PET-Boron Neutron Capture Therapy System

This PET study using ^{18}F-^{10}B-FBPA suggests that ^{10}B-BPA is a compatible boron compound to overcome lack of success in early BNCT (*1–3*). The uptake of this boron compound was thought to be strictly controlled by a transport system involved by amino acid transport and it achieved selective localization in the tumor. The indications for BNCT vary greatly among individual cases. When determining dosimetry of BNCT, the depth of tumor and the uptake of boron compounds are important. The ability to incorporate boron compounds differs greatly even when the grade of brain tumor is the same (Table 1). It is necessary to know the tumor ^{10}B levels accurately, either before or shortly after starting neutron application. If the rate constants are used, it will be possible to predict tumor ^{10}B levels before BNCT treatment by measurement of blood ^{10}B levels immediately before starting the therapy (*22*). Preliminary data about the correlation suggested that incorporated L-^{10}B-BPA per total injection dose estimated by inductively coupled plasma-atomic emission spectroscopy corresponds almost 1:1 to the L-^{18}F-^{10}B-FBPA estimated by the specific activity (*8,11,23*). These results formed the basis for the concept of a PET-BNCT system. We have estimated brain tumor ^{10}B levels using the rate constants of L-^{18}F-^{10}B-FBPA obtained in this study. This estimation used the subtherapeutic dose level of L-^{10}B-BPA for BNCT. The estimated value was very close to the ^{10}B level actually measured in surgical specimens (*24*). The rate constants presented here are, therefore, expected to serve as important factors when BNCT is performed. The system will allow direct study of human glioma with regard to the numerical relationships of the radioactivity of L-^{18}F-^{10}B-FBPA and chemical elements of L-^{10}B-BPA and will be useful to predict the effectiveness of BNCT.

CONCLUSION

The PET data revealed that ^{18}F-^{10}B-FBPA was selectively incorporated to the malignant tumor cells showing high radioactivity and T/N ratio. A three-compartment model using rate constants (K1, k2 and k3) was used for kinetic analysis. The kinetic analysis demonstrated that K1 was closely related to ^{18}F-^{10}B-FBPA uptake, which correlates with the degree of malignancy, and the L form of ^{18}F-^{10}B-FBPA was taken up better by tumor tissue than was its DL form. These PET data will be of practical use for diagnosis of malignancy and direct prediction of the effectiveness of BNCT using ^{10}B-BPA.

ACKNOWLEDGMENTS

This work was supported in part by Grants-in-Aid for Science Research (06282254, 06671411, 07274259 and 8671602) from the Ministry of Education Science and Culture of Japan. We acknowledge the technical support and effort of Kazuo Wakita and Hitoshi Horii (Cyclotron Unit, Nishijin Hospital, Kyoto, Japan). We thank Dr. Kiichi Ishiwata (PET Center, Tokyo Metropolitan Institute of Gerontology) for helpful advice on ^{18}F-^{10}B-FBPA synthesis and its biological properties.

REFERENCES

1. Barth RF, Soloway AH, Fairchild RG. Boron neutron capture therapy of cancer. *Cancer Res* 1990;50:1061–1070.
2. Flam F. Cancer treatment: will history repeat for boron capture therapy? *Science (Washington, DC)* 1994;265:468–469.
3. Asbury AK, Ojemann RG, Nielsen SL, Sweet WH. Neuropathologic study of fourteen cases of malignant brain tumor treated by boron-10 slow neutron capture radiation. *J Neuropathol Exp Neurol* 1972;31:278–303.
4. Hatanaka H. Experience of boron-neutron capture therapy for malignant brain tumors with special reference to the problems of postoperative CT follow-ups. *Acta Neurochir Suppl* (Wien) 1988;42:187–192.
5. Coderre JA, Joel DD, Micca PL, Nawrocky MM, Slatkin DN. Control of intracerebral gliosarcomas in rats by boron neutron capture therapy with p-boronophenylalanine. *Radiat Res* 1992;129:290–296.
6. Coderre JA. A Phase I biodistribution study of p-boronophenylalanine. In: Gabel D, Moss R, eds. *Boron neutron capture therapy: toward clinical trials of glioma treatment*. New York: Plenum Press; 1993:111–121.
7. Mishima Y, Honda C, Ichihashi M, et al. Treatment of malignant melanoma by single thermal neutron capture therapy with melanoma-seeking ^{10}B-compound. *Lancet* 1989;ii:388–389.
8. Imahori Y, Ueda S, Ohmori Y, et al. A basic concept for PET-BNCT system. In: Mishima Y, ed. *Cancer neutron capture therapy*. New York: Plenum Press; 1996: 691–696.
9. Ueda S, Imahori Y, Ohmori Y, et al. Positron emission tomography and boron neutron capture therapy system to the patient with malignant brain tumor: the first clinical trial using ^{10}B-BPA. In: Mishima Y, ed. *Cancer neutron capture therapy*. New York: Plenum Press; 1996:823–827.
10. Ishiwata K, Ido T, Mejia AA, et al. Synthesis and radiation dosimetry of 4-borono-2-[^{18}F]fluoro-D,L-phenylalanine: a target compound for PET and boron neutron capture therapy. *Appl Radiat Isot* 1991;42:325–328.
11. Mishima Y, Imahori Y, Honda T, Hiratsuka J, Ueda S, Ido T. In vivo diagnosis of human malignant melanoma with positron emission tomography using specific melanoma-seeking ^{18}F-DOPA analog. *J Neuro Oncol* 1997;33:163–169.
12. Phelps ME, Huang S-C, Hoffman EJ, Kuhl DE. Validation of tomographic measurement of cerebral blood volume with C-11-labeled carboxyhemoglobin. *J Nucl Med* 1979;20:328–334.
13. Wienhard K, Herholz K, Coenen HH, et al. Increased amino acid transport into brain tumors measured by PET of L-(2-^{18}F)fluorotyrosine. *J Nucl Med* 1991;32:1338–1346.
14. Patlak CS, Blasberg RG, Fenstmacher JD. Graphical evaluation of blood-to-brain transfer constants from multiple-time uptake data. *J Cereb Blood Flow Metab* 1983;3:1–7.
15. Huang S-C, Phelps ME, Hoffmann EJ, et al. Non-invasive determination of local cerebral metabolic rate of glucose in man. *Am J Physiol* 1980;238:E69–E82.
16. Ishiwata K, Ido T, Kawamura M, et al. 4-Borono-2-[^{18}F]fluoro-D,L-phenylalanine as a target compound for boron neutron capture therapy: tumor imaging potential with positron emission tomography. *Nucl Med Biol* 1991;18:745–751.
17. Tylor JL, Diksic M, Villemure J-G, et al. Metabolic and hemodynamic evaluation of gliomas using positron emission tomography. *J Nucl Med* 1987;28:1123–1133.
18. Willemsen ATM, Van Waarde A, Paans AMJ, et al. In vivo protein synthesis rate determination in primary or recurrent brain tumors using L-[1-^{11}C]tyrosine and PET. *J Nucl Med* 1995;36:411–419.
19. Keen RE, Barrio JR, Huang S-C, et al. In vivo cerebral protein synthesis rates with leucyl-transfer RNA used as a precursor pool: determination of biochemical parameters to structure tracer kinetics models for positron emission tomography. *J Cereb Blood Flow Metab* 1989;9:429–445.
20. Yoshino K, Mori Y, Kakihana H, et al. Chemical modeling with p-boronophenylalanine for boron accumulation to and release from melanoma. In: Mishima Y, ed. *Cancer neutron capture therapy*. New York: Plenum Press; 1996:81–90.
21. Guidotti GG, Gazzola GC. Amino acid transporters: systematic approach and principles of control. In: Kilberg MS, Haussinger D, eds. *Mammalian amino acid transport: mechanisms and control*. New York: Plenum Press; 1992:3–29.
22. Imahori Y, Ueda S, Ohmori Y, et al. Boron neutron capture therapy: ^{18}F-labeled fluoroboronophenylalanine and its pharmacokinetics in patients with gliomas [Abstract]. In: Larsson B, ed. *Seventh international symposium on neutron capture therapy for cancer*. Zurich: PSI; 1996:89–90.
23. Ishiwata K, Shiono M, Kubota K, et al. A unique in vivo assessment of 4-[^{10}B]borono-L-phenylalanine in tumor tissues for boron neutron capture therapy of malignant melanomas using positron emission tomography and 4-borono-2-[^{18}F]fluoro-L-phenylalanine. *Melanoma Res* 1992;2:171–179.
24. Ueda S, Imahori Y, Ohmori Y, et al. Positron emission tomography: boron neutron capture therapy system and its clinical application to patients with malignant gliomas [Abstract]. In: Larsson B, ed. *Seventh international symposium on neutron capture therapy for cancer*. Zurich: PSI; 1996:164.